A Cascade Tunnel for Investigation of Rotating Stall

A. R. KRIEBEL

A. H. STENNING

REPORT NO. 26

GAS TURBINE LABORATORY
MASSACHUSETTS INSTITUTE OF TECHNOLOGY
CAMBRIDGE · 39 · MASSACHUSETTS

A CASCADE TUNNEL
FOR INVESTIGATION OF
ROTATING STALL

A. R. KRIEBEL

A. H. STENNING

NATIONAL ADVISORY COMMITTEE FOR AERONAUTICS

CONTRACT NAw-6303

DIC 7119

"STALL FLUTTER PHENOMENA IN AXIAL FLOW MACHINES"

TERMINAL REPORT

JUN 1954

GAS TURBINE LABORATORY REPORT NO. 26

MASSACHUSETTS INSTITUTE OF TECHNOLOGY

CAMBRIDGE, MASS.

ABSTRACT

A test apparatus which will reproduce the rotating stall phenomenon found in axial compressors has been constructed and installed in the main wind tunnel circuit of the Gas Turbine Laboratory.

The test secion consists of a two dimensional, circular, radial outflow cascade between two flat plates. The cascade was designed to reproduce the pressure distribution, and hence the stall characteristics, of a typical rectilinear cascade.

The air entry angle to the cascade is controlled by a variable angle nozzle ring so that the cascade may be stalled and unstalled in operation. Provision has been made for removal of wall boundary layers by suction, and for changing the setting of the cascade stagger angle. By a simple modification, the blades may be supported elastically to permit torsional vibrations. Independent variation of the Reynolds number and Mach number of the air stream is possible.

Visual observations of the flow using Schlieren and Interferometer equipment can be made through windows in the walls of the test section.

In preliminary tests, rotating stall has been observed and the research program will commence in August of 1954.

INTRODUCTION

The problem of compressor blade vibration has received a great deal of study in recent years, with attention focussed on the possible sources of excitation. Stall flutter was for some time considered to be the prime cause of blade failures, but with the discovery of the phenomenon of rotating stall the emphasis has shifted away from flutter, although the possibility of vibrations excited by rotating stall and amplified by flutter cannot be neglected.

The existing theories of rotating stall (ref. 1, 2, 3, 4) rely on assumptions regarding the nature of the process of boundary-layer separation and reattachment which are frequently conflicting and are as yet unsubstantiated. In consequence, it is highly desirable to be able to study closely the changes in the flow about individual airfoils, under conditions similar to those in turbo-machines.

Most investigations of rotating stall have been carried out with rotating machinery (ref. 1, 5, 6) and this method of attack suffers from the disadvantage that the mechanism of the stalling process cannot be examined. Professor H. W. Emmon's group at Harvard have studied stall propagation in a rectilinear cascade (ref 1), using Schlieren apparatus; but, due to the finite length of the cascade, stalled regions appeared at random intervals rather than periodically and end effects may have had an influence on the velocity of propagation of the stall cells.

It appears, therefore, that to examine the details of stall propagation under conditions resembling those found in axial compressors, some form of circular cascade is required. To avoid the spanwise variations in geometry found in an annular cascade and to facilitate optical observation, a plane, two dimensional flow is desirable so that the cascade should be of either

the radial outflow, or radial inflow configuration.

In this report a test apparatus of this type is described and the main results of the calculations used in the design are summarised.

THE TEST APPARATUS

I Preliminary Design Considerations

The main requirements of the apparatus were, that it should consist of a circular cascade of airfoils with provisions for varying the air entry angle continuously while operating, and that observation by means of the Gas Turbine Laboratory portable Schlieren or Interferometer equipment (shown in Figures 7 and 8) should be possible.

The configuration adopted was a double-entry, radial outflow type, with the air inlet angle to the cascade controlled by means of a stationary, variable-angle nozzle ring. A schematic diagram is given in Figure 1 and photographs of the apparatus and of the test section are shown in Figures 2, 3 and 4. Figures 5 and 6 show assembly drawings of the test section and the complete rig. The airstream is collected in a scroll for return to the wind tunnel circuit after passing through the nozzle ring, the test cascade, and a short vaneless diffuser.

This configuration permits an unobstructed airstream ahead of the nozzle ring. A source-type of radial outflow is easily attained by means of impingement of two airstreams. It is important to have the inlet pipes as small as possible to facilitate mounting the interferometer around the cascade, but the inlet pipe cross sectional area must be equal to or greater than the annulus area of the cascade, otherwise adverse pressure gradients and the likelihood of flow separation from the walls of the divergent portion of the inlet section results.

The following methods for supplying the airstream were considered and discarded for the reasons indicated.

1.) Radial inflow - Compared to outward flow it is difficult to obtain a uniform radial velocity around the circumference of the cascade entry. A more elaborate and expensive scroll would undoubtedly

be necessary.

2.) Radial outflow with one inlet pipe - The inlet pipe diameter in this case would be so large in comparison to the cascade diameter for reasonable blade lengths that the interferometer could not be fitted around the apparatus.

The following methods for varying the air inlet angle to the test cascade were considered and discarded for the reasons indicated.

1.) Radial inflow to test cascade with variable angle compressor blades - Difficulty would be encountered in turning blades mounted in the test windows without obscuring them from view. It would also be more difficult to maintain a close tolerance on blade setting if the blades could be rotated than if they were rigidly mounted.

2.) Variable speed rotor before test cascade - The bearings of the rotor would interfere with the entering airstream. To provide or dissipate approximately 100 HP which would be required to turn the airstream through the required range of angles would present a serious problem. Furthermore, unsteady flow effects due to passing rotor blades would complicate the interpretation of the test data.

II Size Considerations

For the largest number of constant density interference bands to appear in the interferogram, maximum values of the following quantities are desirable.

1.) Mach number through the cascade

2.) Blade length

3.) Density level

Maximum blade length is also desirable to minimize the ratio of wall boundary layer thickness to blade length. Maximum cascade radius is desirable for fitting the interferometer around the apparatus.

The upper limit of each of these quantities is set by the characteristics of the compressor-motor combination of the air supply. Mach number and flow area are limited by the volume flow available; the density level is limited by the power available.

It was found that, with inlet stagnation temperature to the compressor held constant, with power maintained at 90 percent of maximum available, with Mach number constant at the entry to the cascade, and with similarly shaped test sections, a decrease in the corrected mass flow through the compressor caused an increase in the number of band shifts available in the interferogram. The lower limit of mass-flow is set by either the point at which the physical dimensions of the test section become so small that the interferometer could not be fitted to it or when the blades become so small and thin that they would be difficult to machine and mount.

The design offers a compromise between these considerations. A summary of the design operating characteristics is as follows:

1.) Mass flow 16.3 lb./sec.

2.) Stagnation pressure before the compressor, 14.5 psia
Stagnation pressure after the compressor, 18.1 psia

3.) Stagnation temperature, 90 F^{o}

4.) Mach number leaving turbine blades, .71

5.) Mach number entering compressor cascade, .59

6.) Properties of linear cascade simulated

a) solidity, chord/pitch, 1.0

b) pressure coeficient at design point

$C_p = 0.46$

c) cascade inlet air angle at design point from radial direction, 48.5^{o}

d) cascade blades with NACA (a = 1.0) mean line cambered design lift coefficient, $C_{l_o} = 1.5$

e) blade dimensions

chord = 1.47 inches = c

length = 1.70 inches = L

aspect ratio = 1.15 = $\frac{L}{c}$

7.) Properties of circular cascade.

a) Limits of the air entry angle are from 30° to 70° from radial

b) At the design point the entry angle is 48.5° and pressure coefficient is 0.46

c) Cascade radius to leading edge = 7.91 inches

d) Three blades are visible in the test window.

III Summary of Calculations

Stagnation pressure losses through the circuit were estimated in order to construct an approximate operating line for the air supply and to find the state of the airstream entering the test cascade. The results of these calculations are indicated in the schematic diagram and table of Figure (9) and the compressor operating map comprising Figure (10).

The number of interferogram band shifts caused by density variation around the blade profile for a magnesium arc light source, inlet Mach number = .6, and the blade in a stalled condition, is estimated at 4.3 bandshifts from the free stream to the stagnation point and approximately 13 total band shifts around the profile. This number of band shifts, although less than optimum for precise interferometric measurement, should clearly indicate the nature of the density field around the blade.

In order to approximate the amount of suction required for removing the boundary layer from the walls of the cascade, an estimation of the boundary layer growth from the inlet screens to the cascade was made. The location of the screens is indicated in Figure 6.

The position of the boundary layer suction slots is shown in Figure 1; an estimated 0.24 lbs sec suction flow is required to remove the boundary layer fluid. This mass flow is well within the capacity of the steam ejector system installed in the Laboratory.

The estimated variation of the normal component of air velocity into the suction slot caused by the spacing of the holes, amounts to less than ten percent of the average normal velocity into the slot. This estimate is conservative since it was assumed that the holes act as point sinks.

Other steps taken in the design to reduce velocity variations, in addition to boundary layer suction, are the use of turning vanes in the bends, straightening tubes, and two screens before each entrance section as indicated in Figure 6. The screens theoretically should reduce the turbulence level of the airstream by a factor of 70 percent and produce flat velocity profiles across the ducts.

The internal shape of the section leading into the cascade of nozzle blades was obtained from a thesis investigation performed at the University of Iowa (ref. 7) which determined the surface generated by the free streamlines of a circular jet of incompressible fluid impinging normally upon a plane. Although the design Mach number of the jet is 0.44 the internal shape based upon an incompressible solution should prove satisfactory in providing approximately uniform pressure on the walls of the entrance section.

The method employed in designing the circular cascade was to transform

by means of mapping function, the straight parallel streamlines of a uniform flow in rectangular coordinates to logarithmic spiral streamlines in a circular plane. In order that the circular cascade might have similar stall characteristics to a linear cascade of compressor blades the reduced adverse pressure gradient $\frac{dp}{d(\frac{x}{c})}$ on the suction side of the blades at the design point was set equal for both cascades. This condition is illustrated in Figure (11) which is a plot of pressure distribution around the blades in the respective cascades.

The system used for setting the pressure gradients equal was as follows:

1) The effect of the transformation upon the pressure gradient was determined.

2) An intermediate linear cascade was determined which would transform to a circular cascade with a pressure gradient equal to that for the original linear cascade.

Equations for the conformal transformation of the uniform flow in rectangular coordinates to a combination source-vortex flow in polar coordinates were obtained from a Gas Turbine Laboratory report by Dr. Charles R. Faulders (ref. 8).

A summary of the results of the calculations follows:

1) Assumed typical linear cascade

Mean line, NACA (a = 1.0)

Camber C_{l_o} = 1.5

Solidity, σ = 1.00

Characteristics of design point

Angle between inlet flow and cascade axis

$\alpha_1 = 48.5^\circ$

Angle between inlet flow and cascade chordline = $i = 16^{\circ}$

Cascade flow turning angle = $\theta = 23.5^{\circ}$

Cascade pressure coefficient = $C_p = 0.46$ as design condition.

2) Properties of intermediate linear cascade.

For an assumed circular cascade radius ratio $R = r_2/r_1 = 1.095$ and an assumed r_1 of 7.91 inches, where r_1 is the leading edge radius and r_2 the trailing edge radius of the cascade, it was found that the circular cascade with $C_p = 0.46$ is transformed from a linear cascade with $C_p = 0.35$.

chord = $c = 1.47$ inches

$C_p = 0.35$

$\sigma = 1.00$

$\alpha_1 = 48.5^{\circ}$

it was found that

$C_{l_o} = .82$

$\theta_1 = 13.5^{\circ}$

$i = 9.5^{\circ}$

3) Properties of the final circular cascade employed in the test section

$r_1 = 7.91$

$R = 1.095$

$C_p = 0.46$

number of blades = 54

Figure (2) is a plot of θ versus α_1 for the original and intermediate cascades. The θ versus α_1 curve for the circular cascade should fall

somewhere between the two linear cascade curves since it was transformed from one and has the same pressure coefficient as the other. Figure (2) indicates that the stalled region of the circular cascade should occure at an angle, α_1, between 45° and 60°.

A cross plot of cascade data from "Fluid Dynamics of Axial Compressors" by A. R. Howell - Proc. of Inst. of Mechanical Engineers, London, Vol. 153, 1945 was found to fall within one degree of the data plotted in Figure (2).

The Reynolds number for the circular cascade based on chord length was found to be approximately 287,000 which is above the lower limit of the data utilized in the design.

From the pressure distribution plot of the blade in the circular cascade, the lift force for one blade was found to be approximately 4.2 lb.

Since the blades in the test cascade are supported by trunnions attached as shown in Figure 5 they may be supported elastically to permit torsional vibrations by a simple modification of the clamping device utilized in the present design.

The blades of the variable angle nozzle ring were designed to provide a continuously accelerating passage for an air exit angle of 50° from radial. This exit angle corresponds to an air entry angle for the test cascade which is 1 $1/2^\circ$ greater than the design air entry angle. The nozzle blades may be turned 20° in either direction from their neutral position by means of a mechanical linkage.

The nozzle and compressor blades are illustrated in Figures 13 and 14.

IV Instrumentation

The quantities to be measured may be divided into two classes:

mean values of pressure, velocity, and flow direction; and instantaneous values of these quantities. The steady state and mean values of static pressure are obtained from static pressure taps placed immediately before and after the nozzles, and before and after the cascade of compressor blades. The windows may be replaced by a traversing gear which permits a total pressure traverse to be made at the entry to the cascade across one passage, and total pressure probes are situated in the pipe just before the nozzle ring. Direction measurements will be made with tufts of thread observed through the windows, although a yawmeter can be fitted if this is found to be desirable. The flow rate in the main circuit and through the suction line may be measured with orifice flow meters.

For the dynamic measurements, several techniques are available. The rotating stall regions can be observed using barium titanate crystals (which detect pressure changes) or with hot-wire instruments, which register velocity fluctuations. The schlieren apparatus is useful for showing qualitatively the changes in the flow pattern, and the density field around the airfoild may be measured with the interferometer. A high speed motion picture camera and a high-speed flash unit with a maximum flash rate of 10,000 per second is available for use with the schlieren and interferometer.

EXPERIMENTAL PROGRAM

In early tests made with the cascade tunnel, rotating stall has been identified using hot wire equipment. The unsteady flow commences at an air inlet angle of approximately 63°, with a frequency which increases with the air inlet velocity from approximately 50 cps at low speed to 100 cps at design speed. A typical oscilloscope trace is reproduced in figure 15.

Spark photographs taken with the schlieren apparatus are shown in figures 16 and 17. In Figure 16, all the airfoils are stalled while in Figure 17, an unstalled region is passing and the center airfoil is unstalled. The oscilloscope trace indicates that the airfoil was stalled for at least 80% of the time period of the oscillation, and the fact that the schlieren photograph shows only one unstalled airfoil suggests that the wave length of the disturbances was approximately 5 blade spacings.

A hot wire probe was installed in the tapered tube upstream of the nozzle ring to detect any velocity fluctuation which might be caused by unsymmetrical flow in the two inlets. While there was rotating stall in the test cascade fluctuations were observed in the tube which were of much smaller amplitude but with the same frequency as those occuring in the cascade. At the design point condition, however, the flow upstream of the nozzles was smooth and no fluctuations in velocity could be detected with the hot wire.

An immediate start is planned on the test program outlined below.

1.) Determination of the performance of the test cascade by measurements of pressure rise and turning angle as a function of angle of attack.

2.) Investigation of the size and velocity of propagation of the

rotating stall regions using hot wire equipment.

3.) Examination of mechanism of the stall process with optical apparatus.

The effect of cascade solidity and stagger on stall characteristics will also be studied.

List of Figures

REFERENCES

1. H. W. Emmons., C. E. Pearson, and H. P. Grant, "Compressor Surge and Stall Propagation". Paper No. 53-A-65. A.S.M.E. December 1953.

2. W. R. Sears, "A Theory of Rotating Stall in Axial-Flow Compressors". Cornell University, January 1953.

3. F. E. Marble, "Propagation of Stall in a Compressor Blade Row". California Inst. of Technology, Janaury 1954.

4. A. H. Stenning, "Stall Propagation in a Cascade of Airfoils". Gas Turbine Laboratory Report No. 25, M.I.T. May 1954.

5. T. Iura and W. D. Rannie, "Experimental Investigation of Rotating Stall in Axial Compressors". Trans. A.S.M.E. April 1954.

6. M. C. Huppert and W. A. Benser, "Some Stall and Surge Phenomena in Axial-Flow Compressors". Journal of the Aeronautical Sciences December 1953.

7. A. Leclere, "Deflection of a Liquid Jet by a Perpendicular Boundary". S.M. Thesis, Graduate College of the State of Iowa. August 1948.

8. C. R. Faulders, "Two Dimensional Incompressible Flow Study of Vaned Diffuser for Centrifugal Compressors". Gas Turbine Laboratory, M.I.T. June 1953.

GLOSSARY

C_p - Cascade pressure coeficient.

C_{l_o} - NACA design lift coefficient.

c - Blade chord.

L - Blade length.

i - Angle between inlet flow and cascade chordline.

r_1 - Radius to leading edge of blade.

r_2 - Radius to trailing edge of blade.

R - Radius ratio $\frac{r_2}{r_1}$.

α_1 - Angle between inlet flow and cascade axis.

σ - Cascade solidity - blade chord/blade spacing.

θ - Cascade flow turning angle.

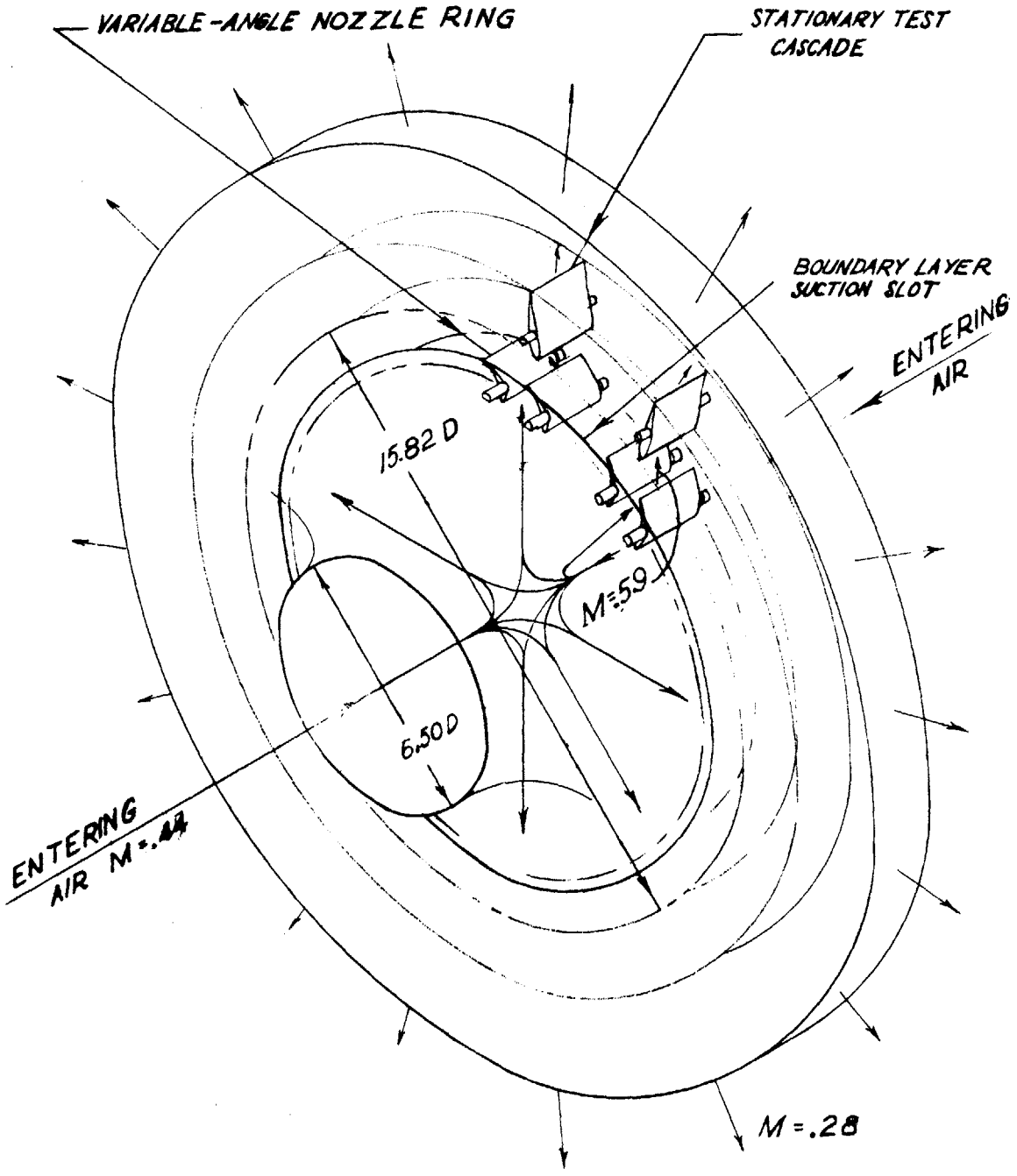

Figure 1. Schematic Diagram of Test Section Configuration

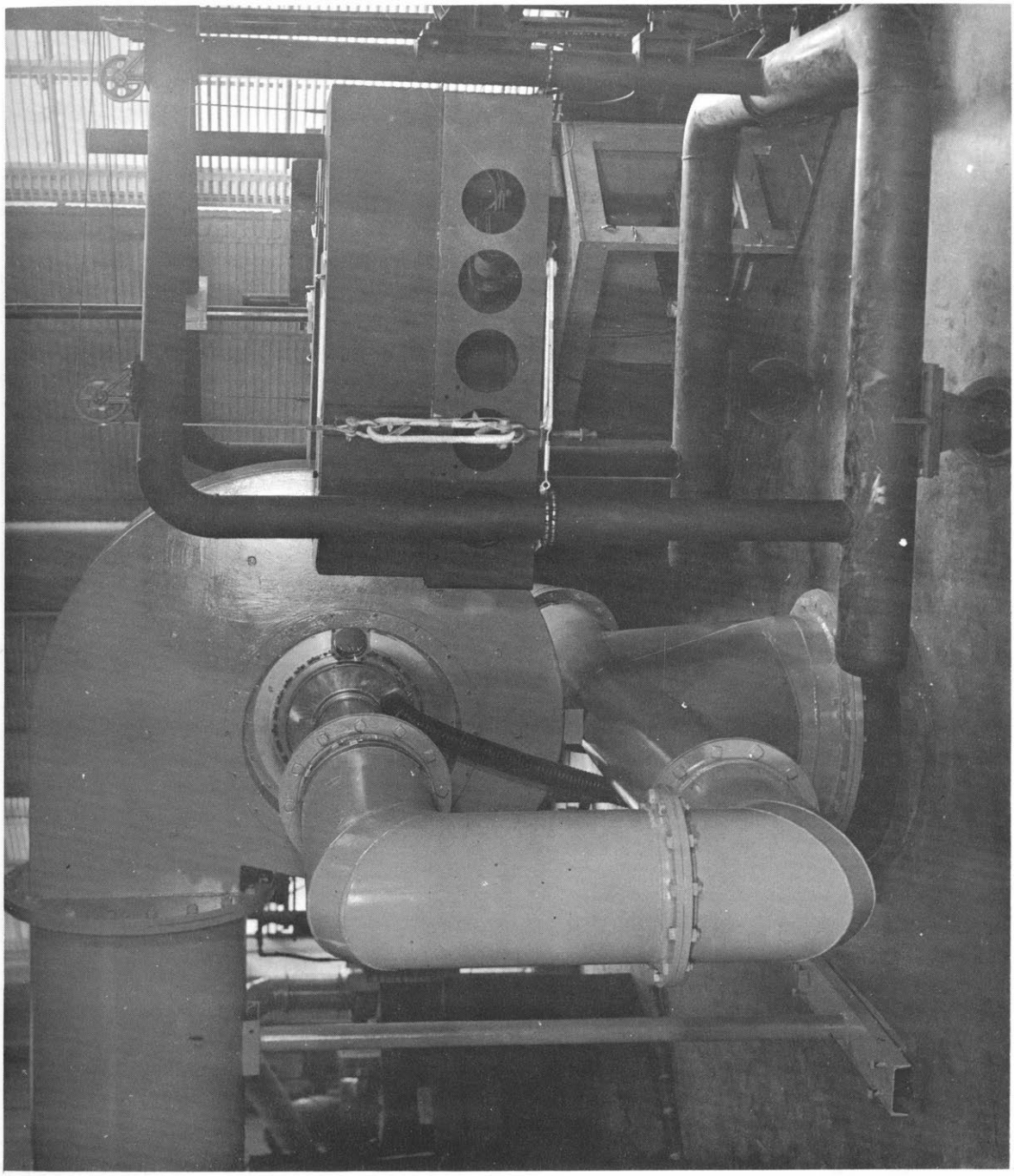

Figure 2. Photograph of Apparatus

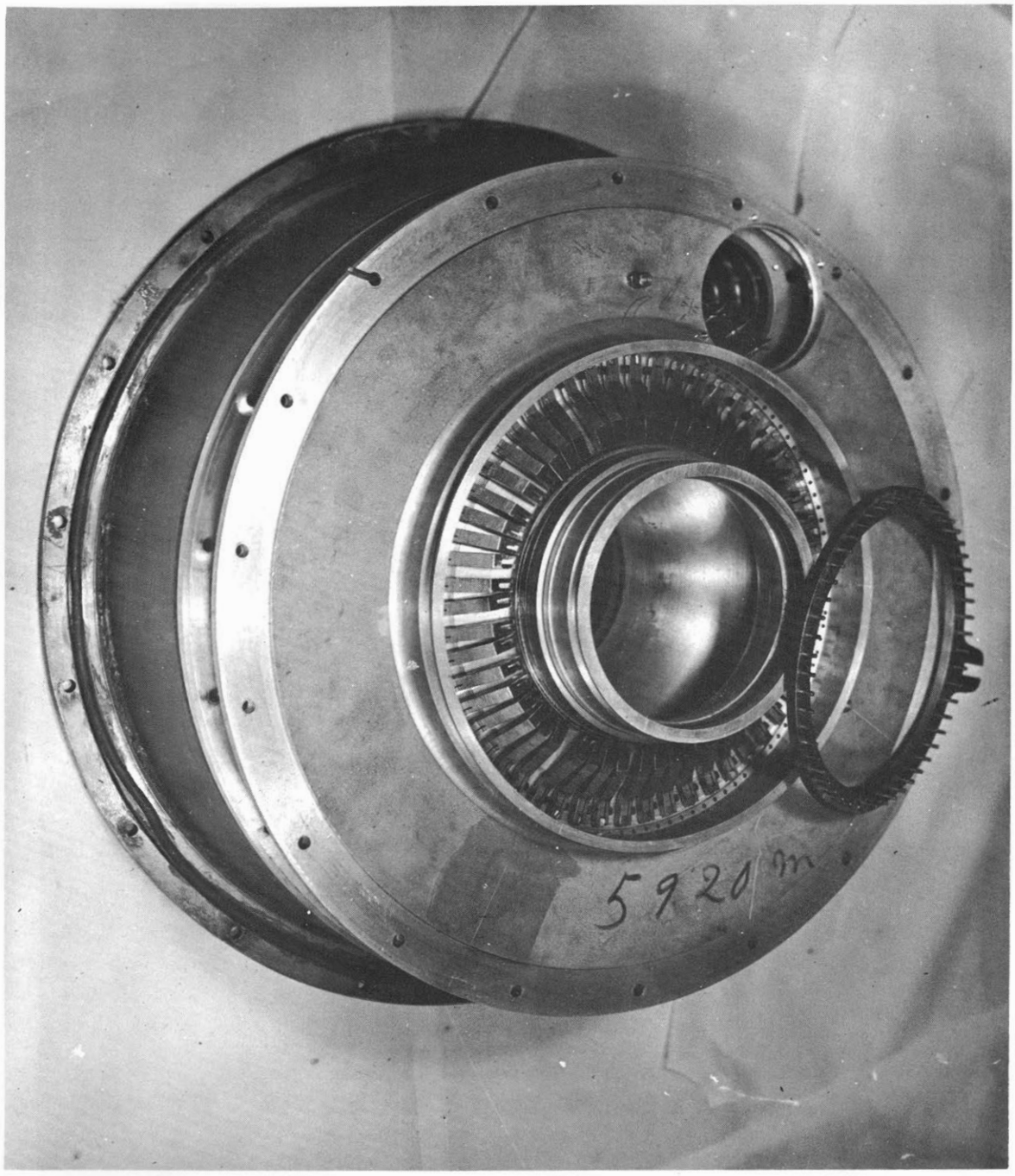

Figure 3. Photograph of Test Section

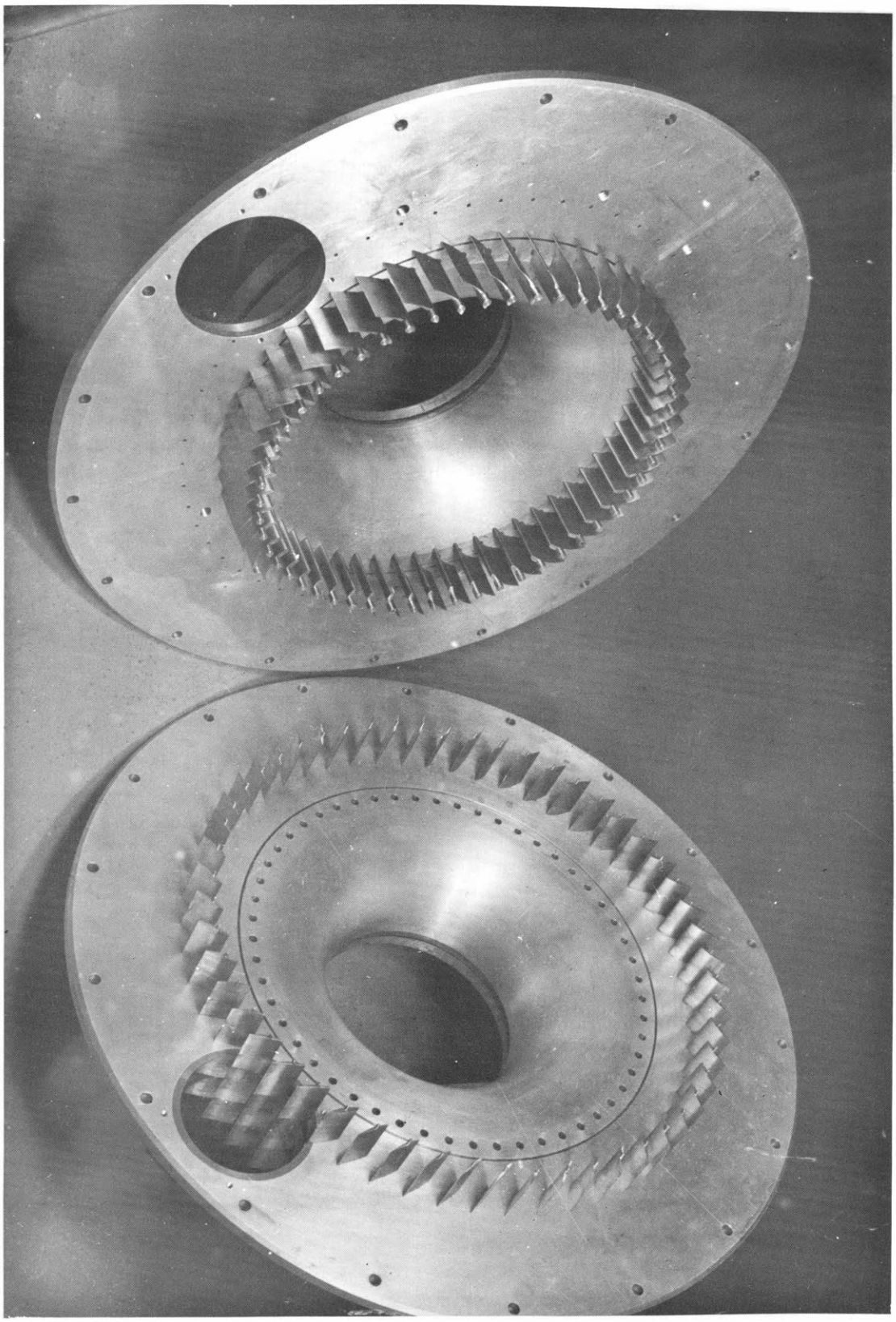

Figure 4. Photograph of Test Section Blading

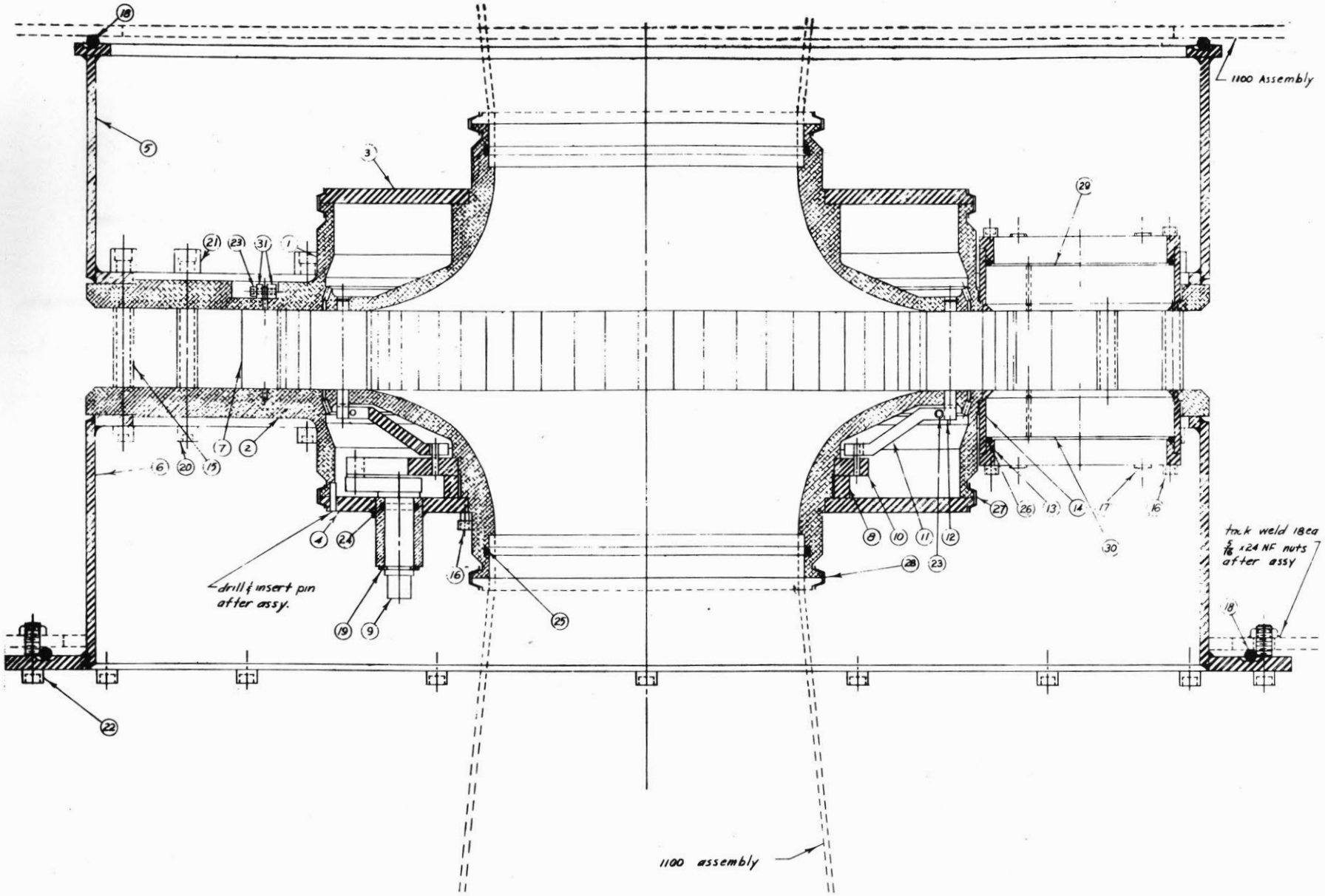

Figure 5. Assembly Drawing of Test Section

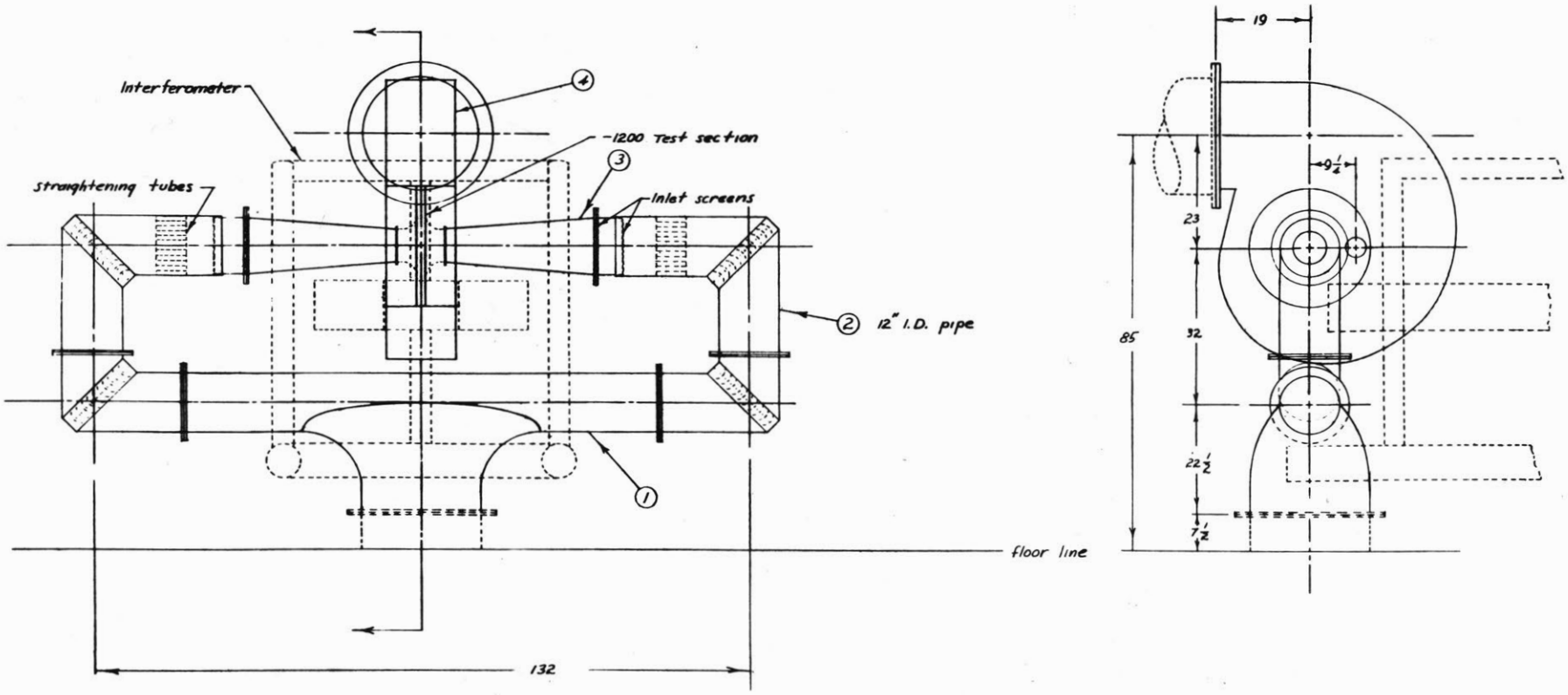

Figure 6. Assembly Drawing of Apparatus

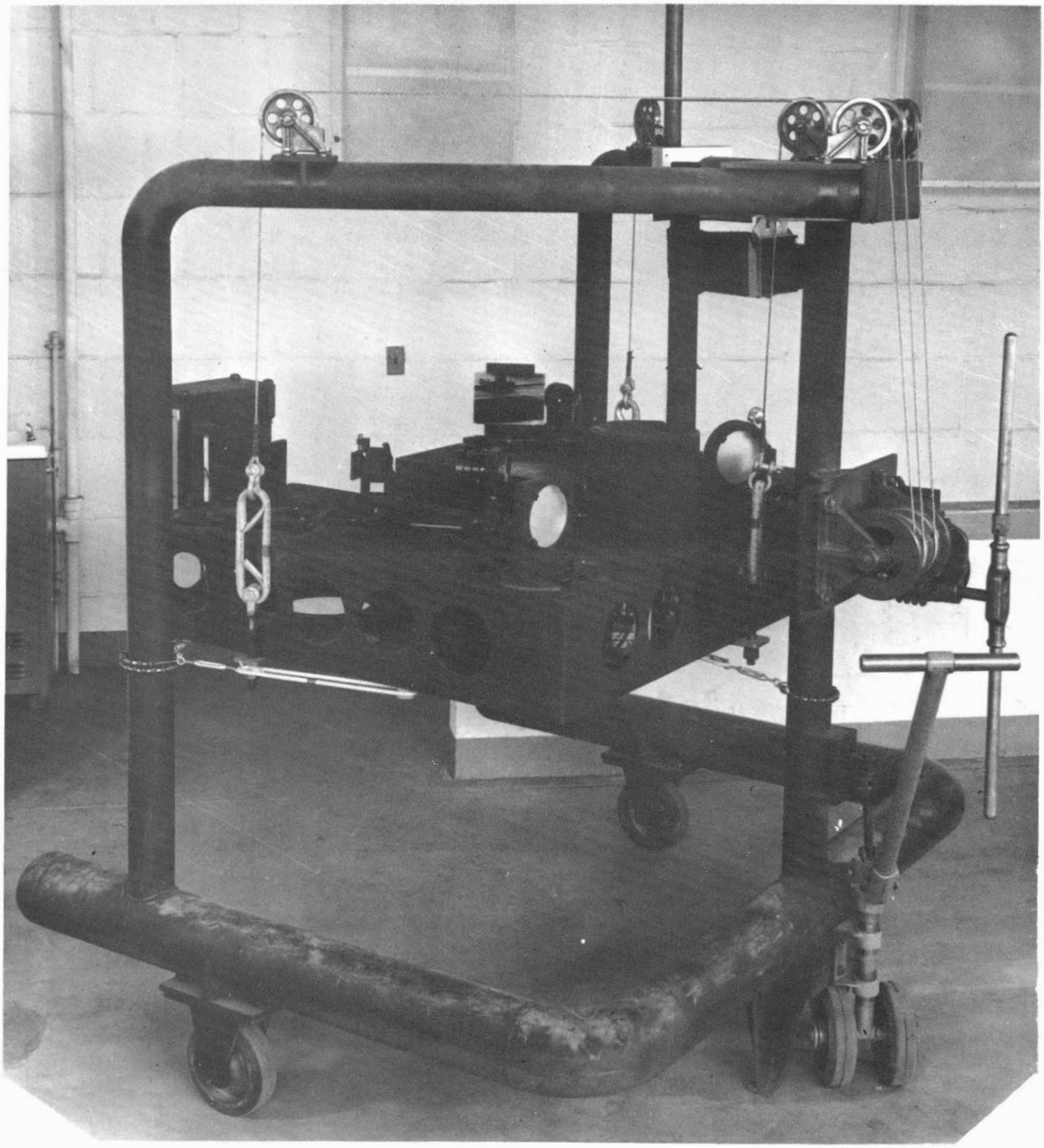

Figure 7. Gas Turbine Laboratory Portable Schlieren

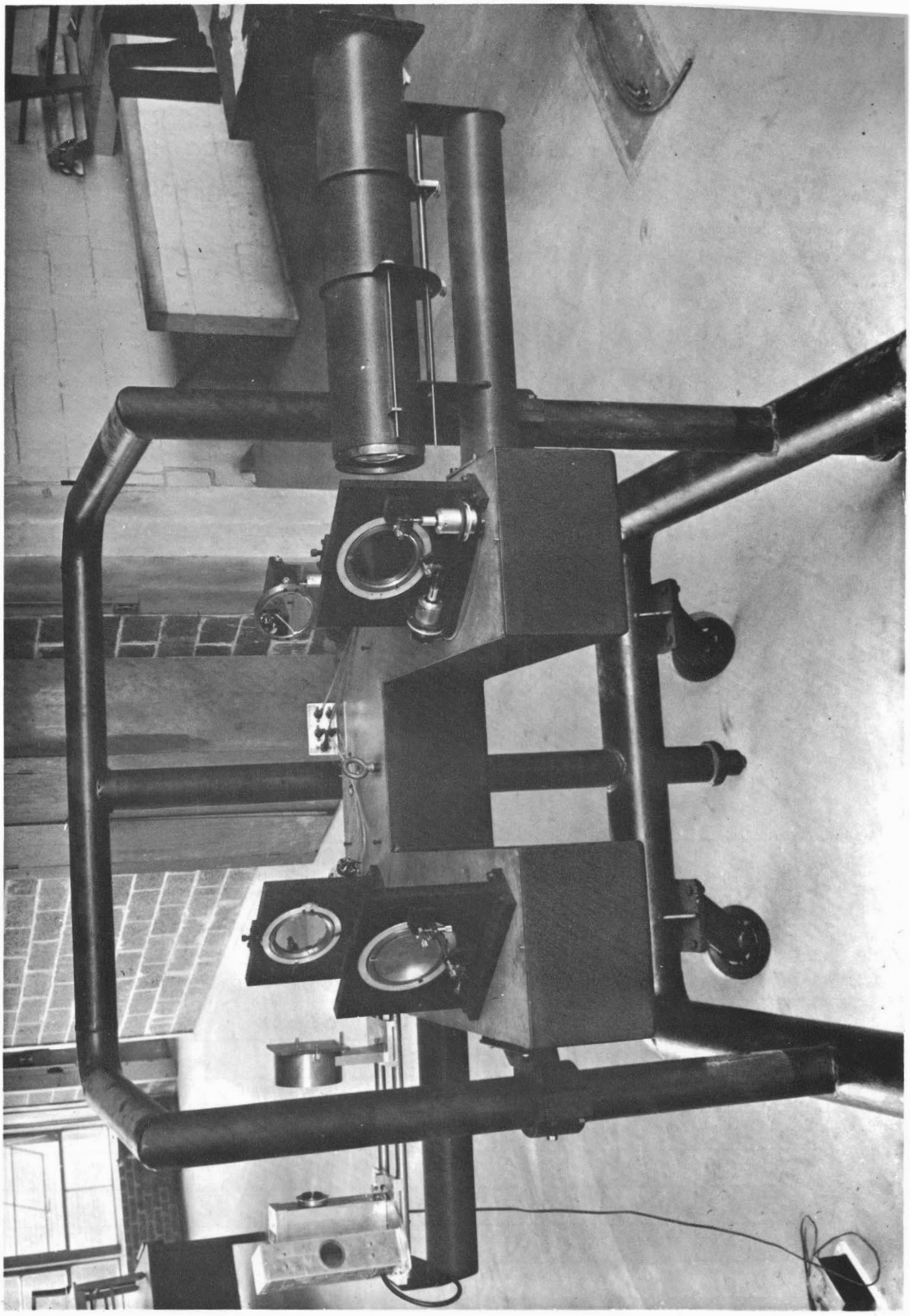

Figure 8. Gas Turbine Laboratory Portable Interferometer

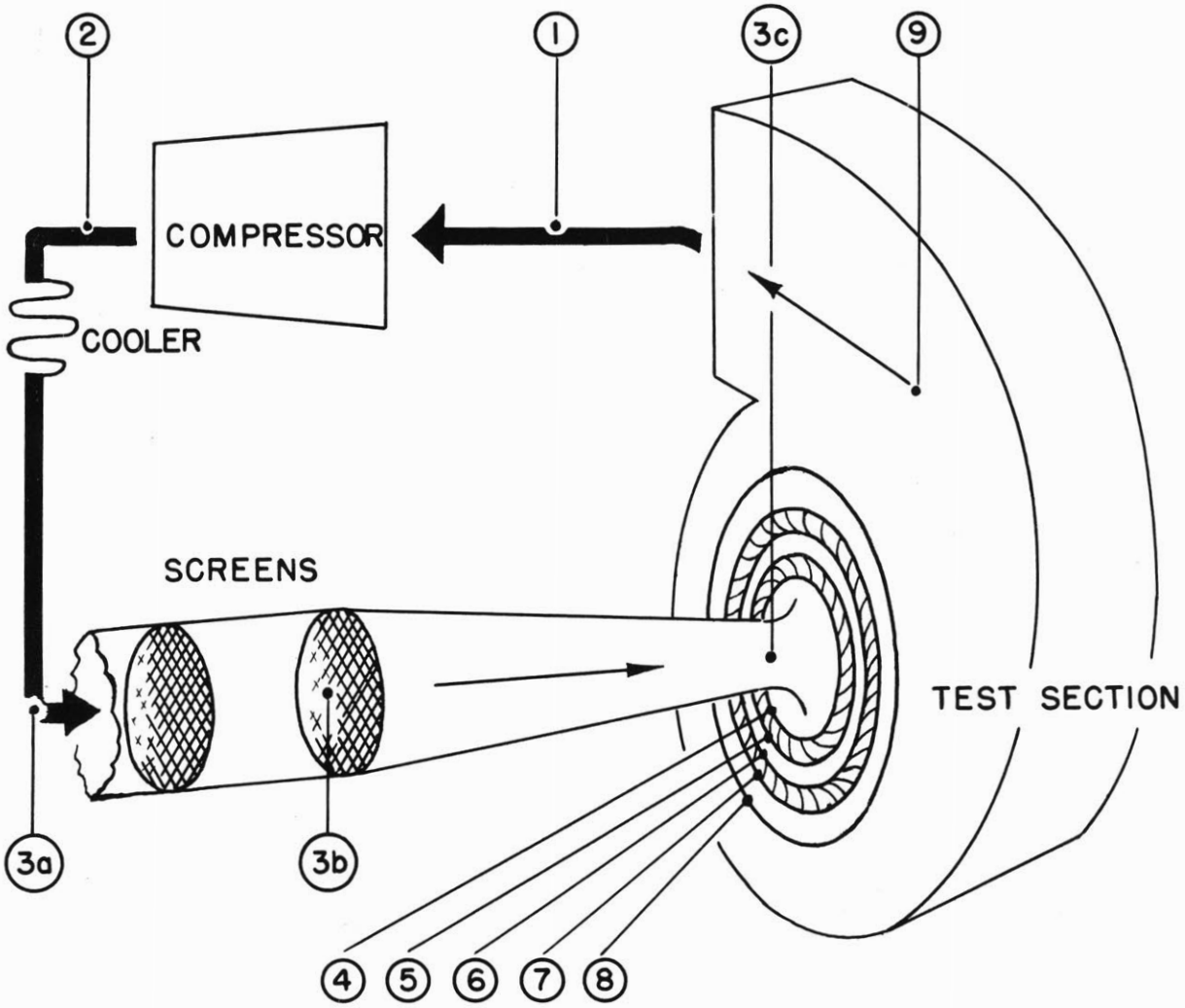

STATION	RADIUS INCH'S	MACH. NO.	VELOCITY F. P. S.	ρ_0 LB-M / FT 3	ρ	P_0 PSIA	P	T °F
1			78	.0712	.0710	14.54	14.49	90
2			62	.0855	.0854	18.09	18.06	90
3a			127	.0814	.0809	16.60	16.47	89
3b			133	.0786	.0781	16.01	15.86	89
3c		.44	498	.0786	.0715	16.01	14.02	70
4	6.0	.45	509	.0786	.0714	16.01	13.93	68
5	7.2	.71	776	.0771	.0608	15.69	11.25	45
6	7.9	.59	658	.0771	.0652	15.69	12.40	54
7	8.7	.39	443	.0759	.0703	15.47	13.93	73
8	12.0	.28	317	.0759	.0730	15.47	14.56	82
9	23.0	.10	115	.0714	.0711	14.56	15.86	89

Figure 9. Air Circuit - Schematic Diagram and Tabulated Properties

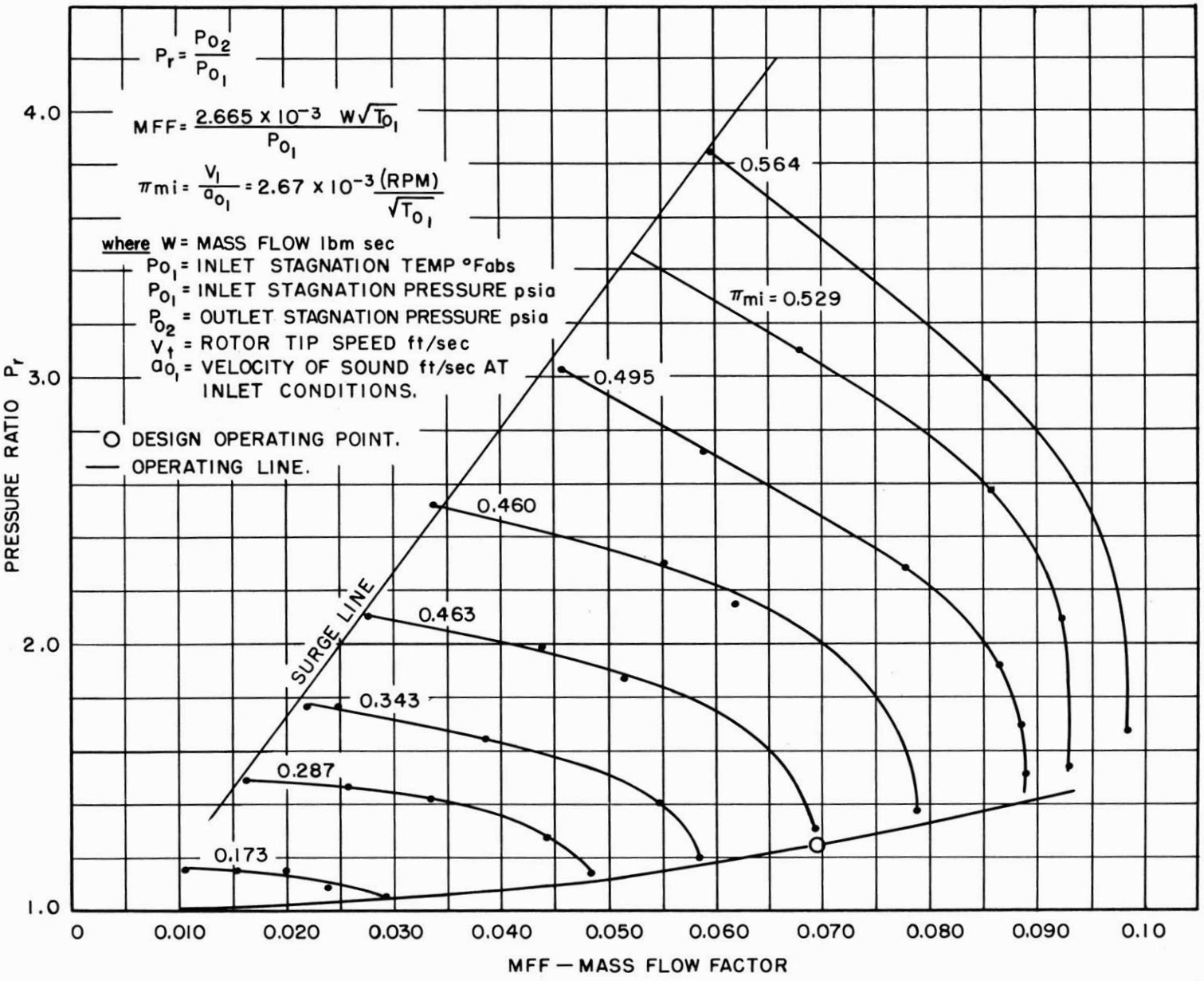

Figure 10. Performance Map of Wind Tunnel Compressor

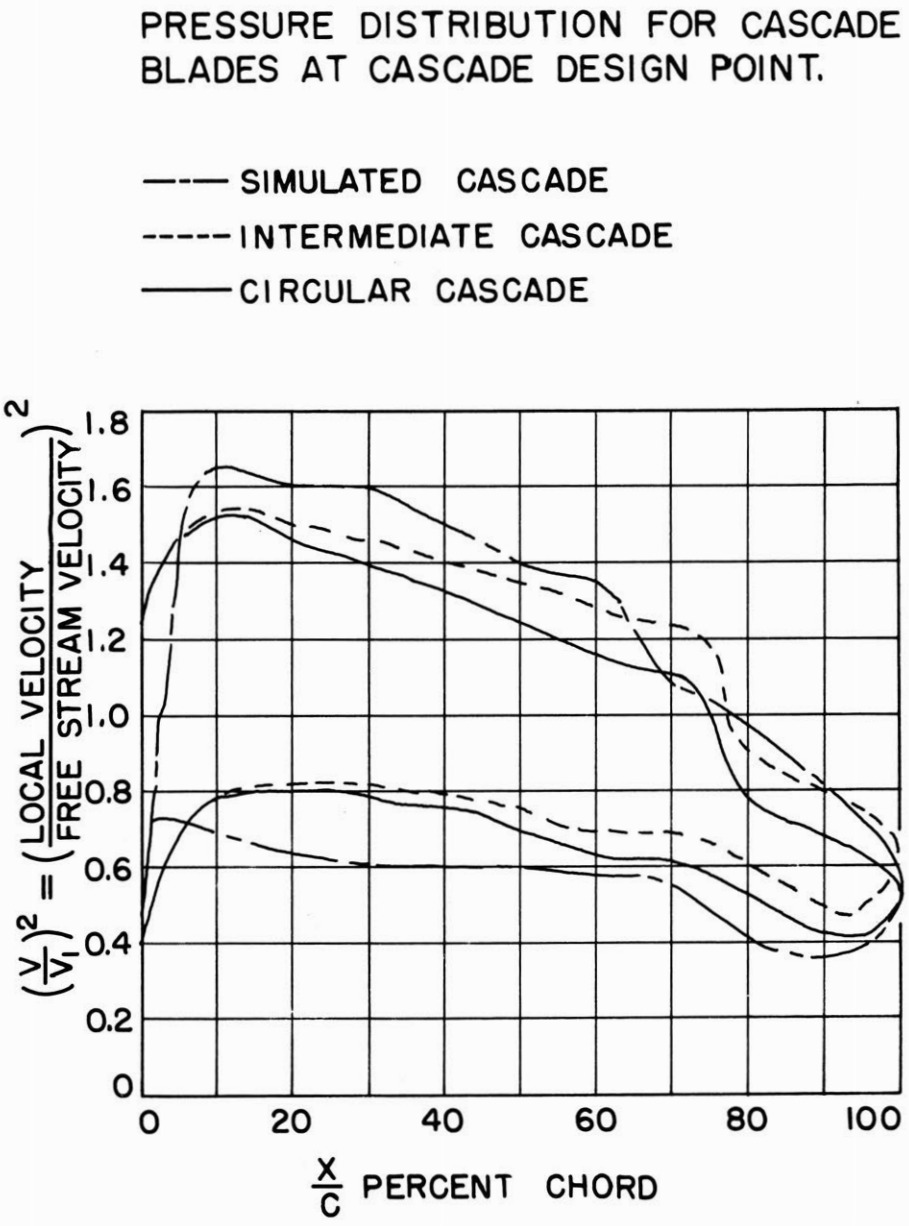

Figure 11. Pressure Distribution for Cascade at Design Point

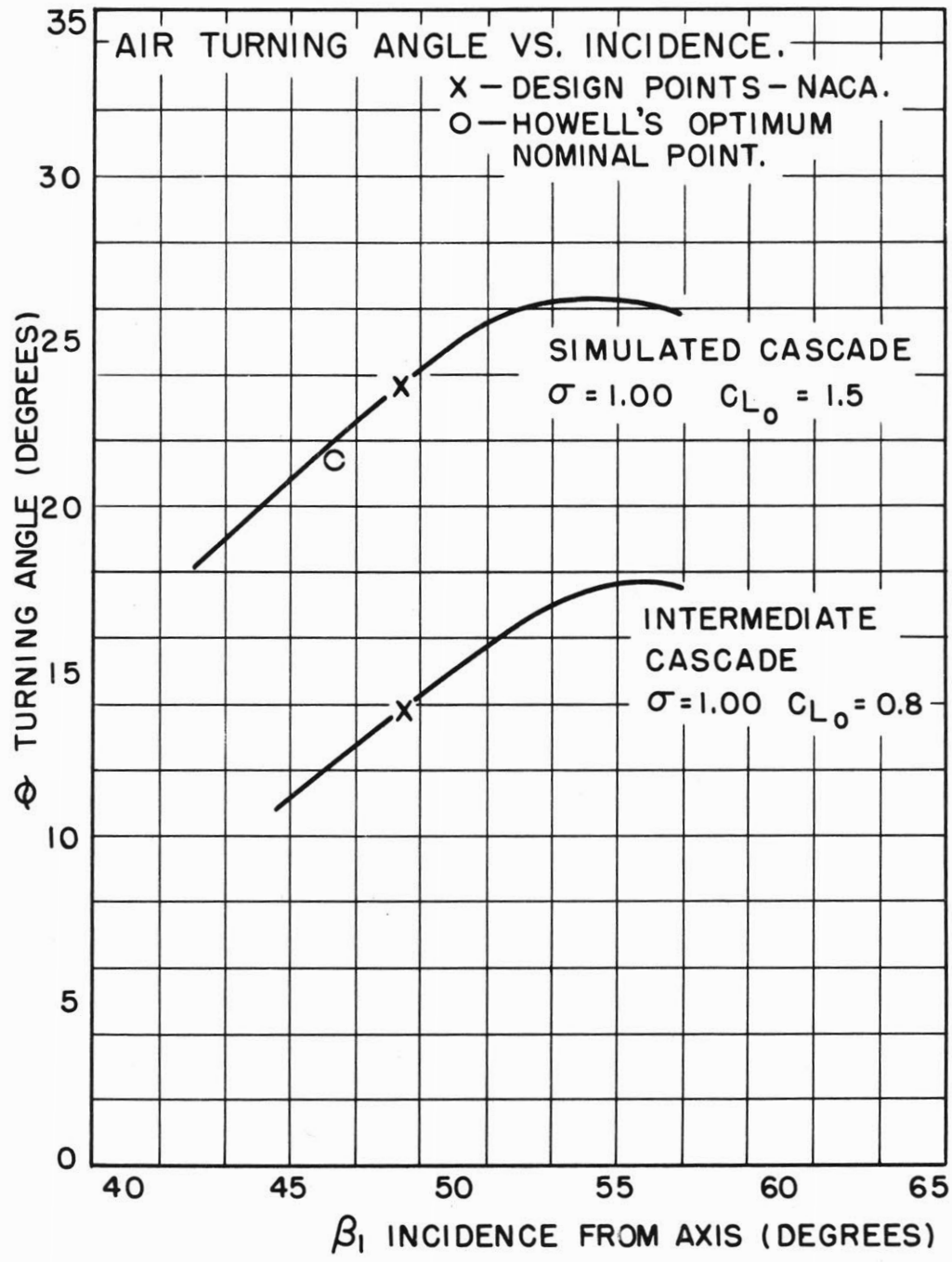

Figure 12. Predicted Cascade Performance

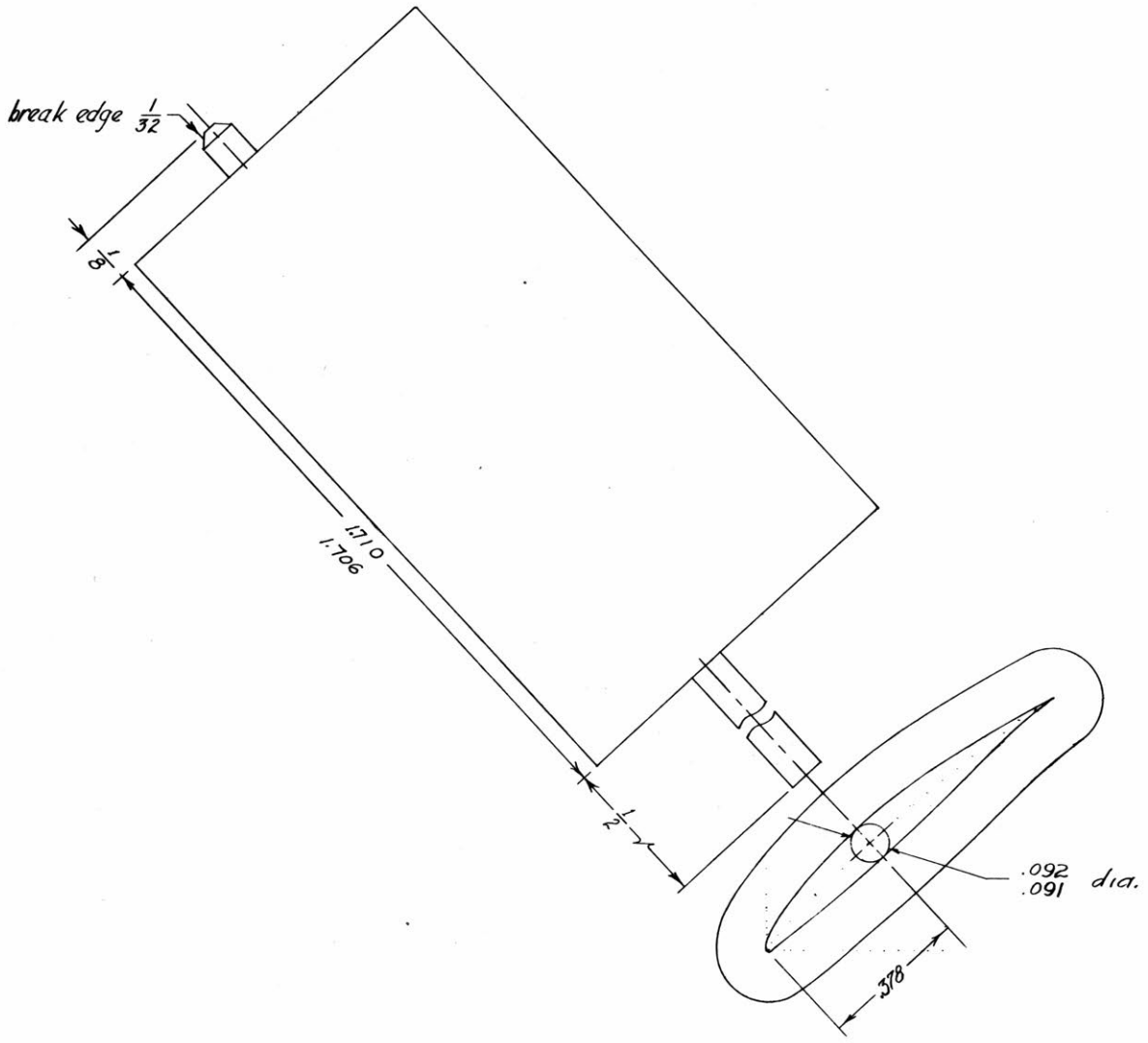

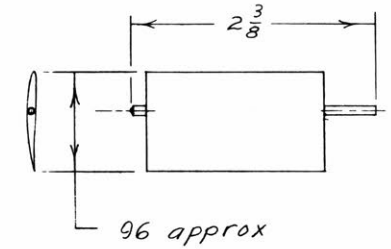

actual size blade

Figure 13. Compressor Blade

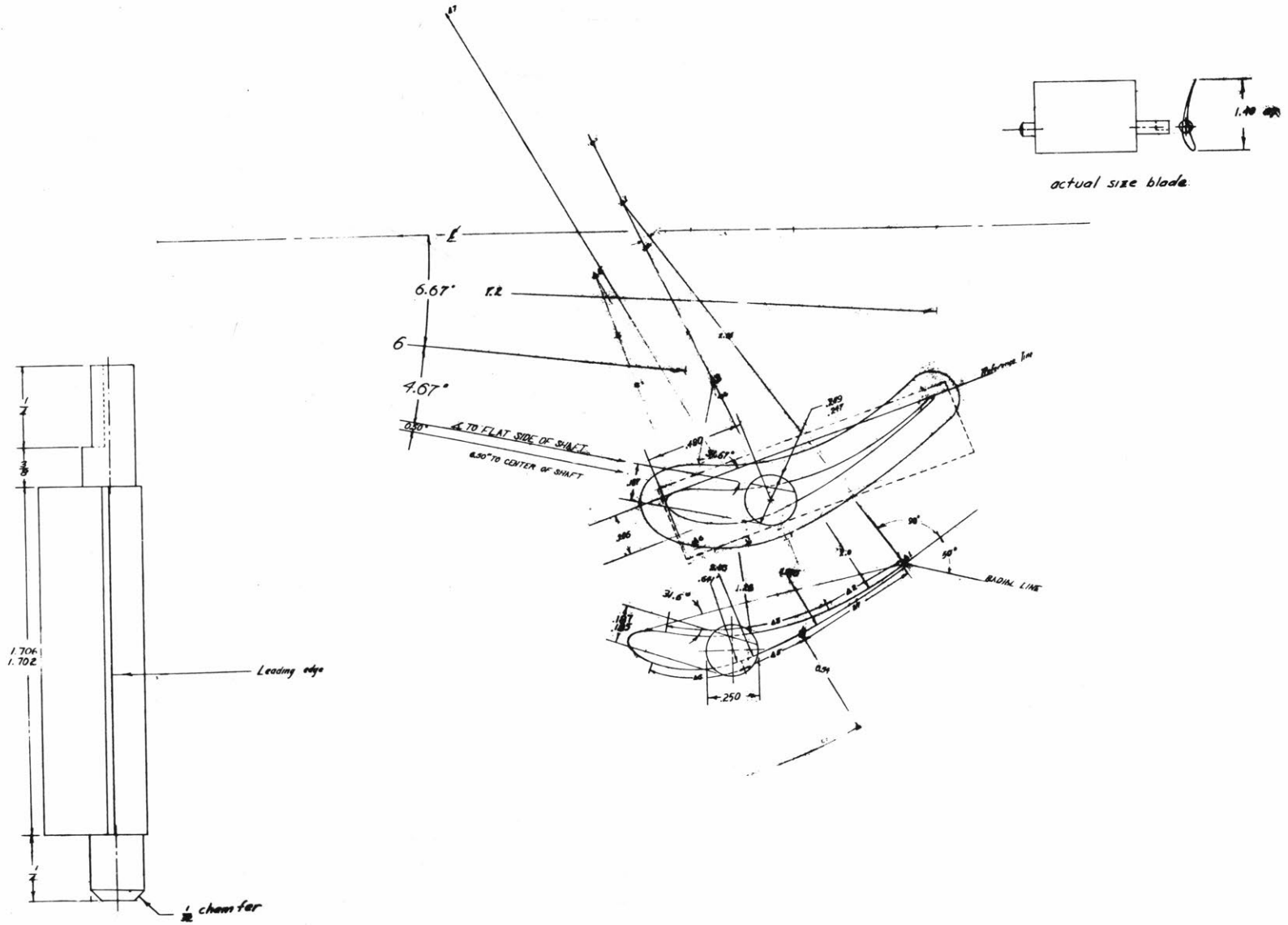

Figure 14. Nozzle Blade

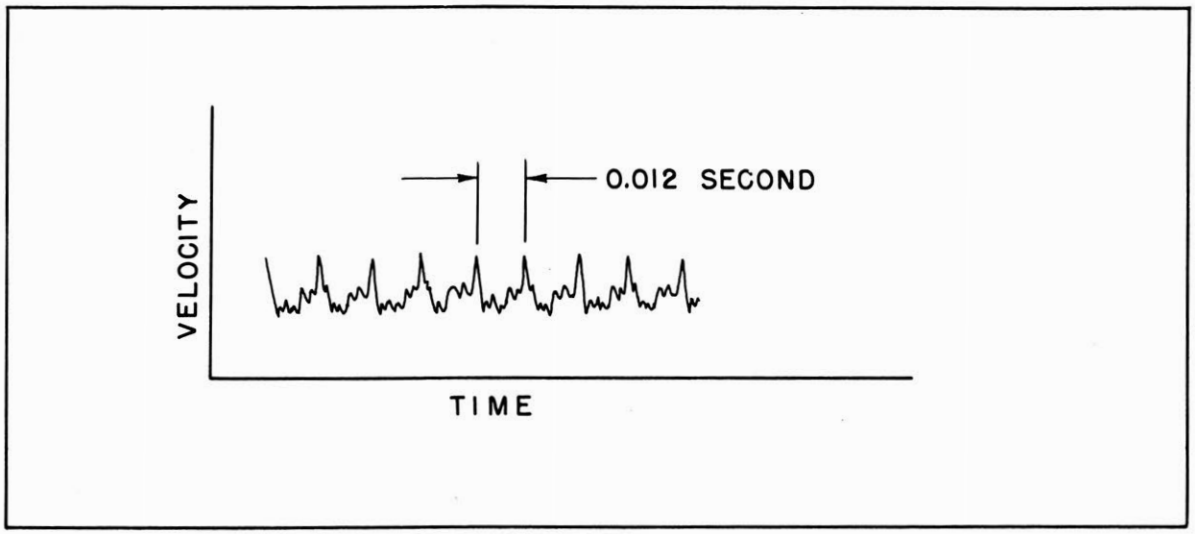

Figure 15. Reproduction of Hot-Wire Trace of Velocity Fluctuation Midway Between Trailing Edges of Two Compressor Blades

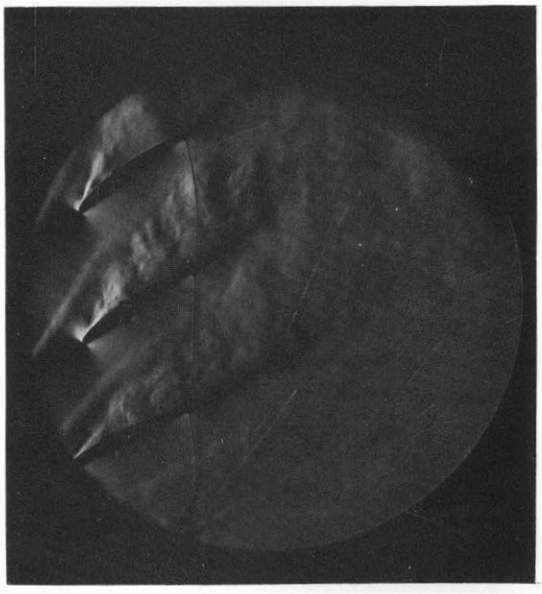

Figure 16. Spark Schlieren Photograph All Blades Stalled

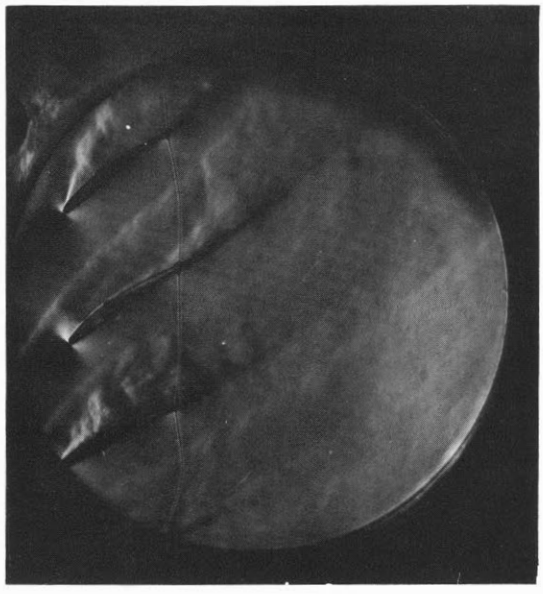

Figure 17. Spark Schlieren Photograph Center Blade Unstalled